Atmospheric electric parameters and micrometeorological processes during the solar eclipse on 15 January 2010

C. P. Anil Kumar,[1] R. Gopalsingh,[1] C. Selvaraj,[1] K. U. Nair,[1] H. Johnson Jeyakumar,[1] R. Vishnu,[2] S. Muralidas,[2] and N. Balan[3]

Received 30 November 2012; revised 17 April 2013; accepted 20 April 2013; published 3 June 2013.

[1] Indian scientists got the unique opportunity to study the near-Earth environment during a long annular solar eclipse at the end of the last long deep solar minimum, on 15 January 2010. Continuous high time resolution records of the atmospheric electric parameters and meteorological parameters were made at Tirunelveli (8.07°N, 77.08°E, 35 m Above Mean Sea Level (AMSL) and Braemore Hill (8.41°N, 76.59°E, 460 m AMSL) stations where the eclipse was during 11:07:57–15:06:52 IST with maximum obscuration (~90%) at 13:17:09 Indian Standard Time (IST). The recorded values of the parameters show marked deviations from those normally observed on control fair-weather days. The ambient electric field underwent a large drop by up to 65% during the eclipse, and potential gradient showed epochs of enhancements during and after the eclipse until postsunset. The data also seem to reveal the long lasting paradox of conductivity enhancement during eclipse, which may be due to the eclipse induced upsurge of low winds or waves that brings high density of free space charges embedded in air parcels.

Citation: Kumar, C. P. A., R. Gopalsingh, C. Selvaraj, K. U. Nair, H. J. Jayakumar, R. Vishnu, S. Muralidas, and N. Balan (2013), Atmospheric electric parameters and micrometeorological processes during the solar eclipse on 15 January 2010, *J. Geophys. Res. Atmos.*, *118*, 5098–5104, doi:10.1002/jgrd.50437.

1. Introduction

[2] Solar eclipses provide an excellent opportunity to study the changes that happen in the near-Earth environment when the solar electromagnetic and corpuscular radiations are suddenly cut off by the transit of the Moon. Excellent studies of atmospheric electric parameters during the past solar eclipses have been made in the Indian subcontinent [e.g., *Kamra and Varshneya*, 1967; *Kamra*, 1982; *Dhanokar et al.*, 1989; *Manohar et al.*, 1995; *De et al.*, 2010; *Deshpande and Kamra,* 1992]. *Kamra et al.* [1982] conducted atmospheric electric field measurements at 0.1, 1, and 2 m heights above the ground at Pune (India) during the solar eclipse of 16 February 1980. They noticed an enhancement in the electric field in the high altitude (2 m) probe during the maximum phase of the eclipse and subsequent negative excursion after the eclipse. *Manohar et al.* [1995] noticed a stepwise drop in the electric potential gradient during the same eclipse, and suggested it as a consequence of the eddy motions during the eclipse.

[3] *Dhanokar et al.* [1989] measured the electric field at the ground in Pune during the eclipse on 18 March 1988 using an AC Field–mill placed in a pit with its sensor flush with the ground, and the conductivity of both polarities were noted with a Gerdian apparatus. They reported an increase in potential gradient, decrease in conductivity, and steady values of conduction current during the eclipse. They also emphasized the need for further study of space charge in the lowest layers of the atmosphere. *Balan et al.* [1982] studied the ionospheric electric field variations at the equatorial station Thiruvananthapuram (India) during the total solar eclipse on 16 February 1980; the associated effects on short wave transmissions were also studied [*Radhakrishnan et al.*, 1982].

[4] Excellent studies during the past solar eclipses around the world have also been reported. For example, *Anderson* [1972] recognized the significance of space charge variations in the lowest few meters of the atmosphere and their influence on the atmospheric electric field and Maxwell current. He also stressed the need to conduct additional measurements at heights of several meters above the ground. *Anderson and Dolezalek* [1972] noticed the currents and electric field recovering back to pre-eclipse levels. They also conducted spectral studies of the space charge, and provided an explanation for the mobility of ions based on the contribution of small ions diffusion during the eclipse. *Szalowski* [2002] studied the air temperature variations near the ground, and seems to confirm the general shape of the temperature curves during eclipses. He also modeled the temperature changes to predict the effect of the solar radiation changes.

[1]Equatorial Geophysical Research Laboratory, Indian Institute of Geomagnetism, Tirunelveli, Tamilnadu, India.
[2]Centre for Earth Science Studies, Thiruvananthapuram, Kerala, India.
[3]Institute of Space Sciences, National Central University, Chung-Li, Taiwan.

Corresponding author: C. P. Anil Kumar, Equatorial Geophysical Research Laboratory, Indian Institute of Geomagnetism, Tirunelveli, Tamilnadu, 627 011, India. (cpanil@iigs.iigm.res.in)

2169-897X/13/10.1002/jgrd.50437

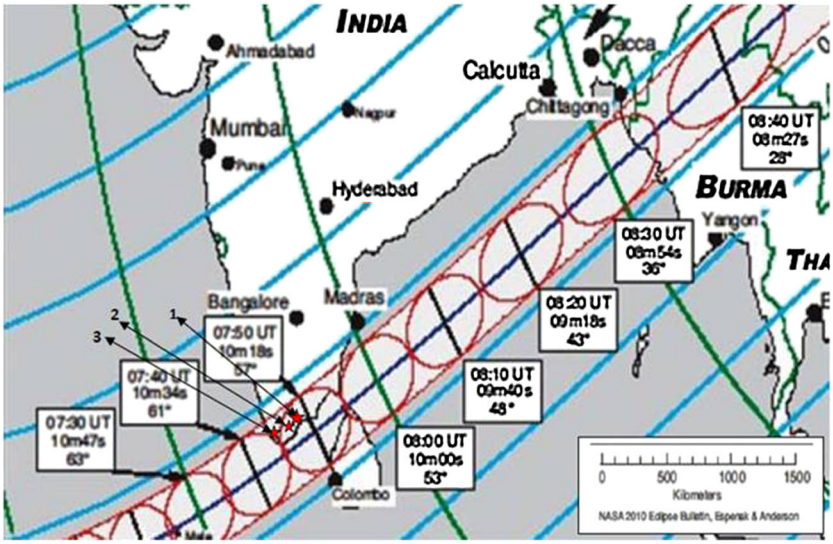

Figure 1. The track (red curves) of the solar eclipse on 15 January 2010 [*Espenak and Anderson*, 2010]; red stars show the observation sites (1) Tirunelveli, (2) Braemore Hills, and (3) Thiruvananthapuram where eclipse was 91%. The red ellipses and square boxes indicate the passage of the eclipse with time in UT.

[5] *Aplin and Harrison* [2003] conducted integrated atmospheric measurements at two stations Camborne and Reading in UK during the total solar eclipse on 11 August 1999. They reported synoptic-scale changes in temperature, wind speed, and direction. With the aid of the UK meteorological network data, *Gray and Harrison* [2012] studied the eclipse-induced wind changes during the total solar eclipse on 11 August 1999. They also reported eclipse-induced atmospheric circulation changes based on a high-resolution weather model. *Farges et al*. [2003] analyzed multistation microbarograph measurements of the atmospheric pressure in the eclipse path in France during the same eclipse on 11 August 1999. They set up multicomponent microbarograph stations to measure the variation of atmospheric pressure on the ground, as well as an ionospheric sounding array. Their measurements showed gravity waves of periods 9–12 min generated in the lower atmosphere during the eclipse. They also found that the gravity waves have only second-order effects on the ionosphere when compared to the 55% decrease of the ionization due to the disappearance of the solar radiation. *Nymphas et al*. [2009] reported the micrometeorological changes observed at Ibadan (Nigeria) during the total solar eclipse on 29 March 2006. A remarkable observation was an upsurge of the wind speed just before the first contact followed by a decrease in the speed.

[6] Some of the specific meteorological features observed in earlier studies include decrease in thermal gradient and increase in pressure gradient, increase in relative humidity, wind chill effect, cloud coverage, eclipse-induced changes in air density, rate of air cooling, decrease of solar UV radiation, and insolation flux during the lunar transit hours [e.g., *Antonia et al*., 1979; *Jones*, 1999; *Chudzynski et al*., 2001; *Szalowski*, 2002; *Aplin and Harrison*, 2003; *Anil Kumar et al*., 2009a; *Nymphas et al*., 2009; *Saxena and Adarsh*, 2010]. Such changes of varying magnitudes and durations in some of the parameters during posteclipse hours were also reported [e.g., *Aplin and Harrison*, 2003].

[7] It is important to collect the data during all solar eclipses for a good understanding of the processes and mechanisms that cause the changes in the near-Earth environment. The present paper reports the high time resolution (1 s sampling) data of the atmospheric electric parameters and meteorological parameters recorded in India during the annular solar eclipse (ASE) at the end of the last long deep solar minimum, on 15 January 2010. An important measurement is the height integrated electric field variation over a wide area on the eclipse path. The eclipse data are compared with the fair-weather data on control days. The important observations are brought out and discussed. This work is a part of the ongoing Global Electric Circuit research being conducted by the Indian Institute of Geomagnetism.

2. Eclipse Track and Observation Sites

[8] The eclipse of 15 January 2010 was one of the longest eclipses, with a total duration of nearly 4 h (05:37:57–09:36:52 UT; 11:07:57–15:06:52 Indian Standard Time (IST)) and maximum obscuration lasting for about 9 min. Figure 1 shows the eclipse track. The central track shown by the red curves is nearly 300 km in width [*Espenak and Anderson*, 2010]. The track traversed nearly half the Earth; it started in Africa, and the central track crossed through the southern peninsular part of India, Bangladesh, Burma, and ended in China. The present measurements are conducted mainly at the Tirunelveli (8.07°N, 77.08°E, 35 m Above Mean Sea Level (AMSL)) and Braemore Hill (8.41°N, 76.59°E, 460 m AMSL) stations (red stars 1 and 2 in Figure 1) where maximum obscuration was 90%. The orography and little aerosol loading in Tirunelveli provided a clear window for the measurements at this station. Braemore Hill station though within the eclipse-geographic grid is located on a hill top.

[9] The Tirunelveli region comes under the monsoon tropics of the southern peninsular part of India. Because the terrain is rocky, less sandy, and rain fall is scanty, the

Table 1. Summary of Meteorological Observations During the Solar Eclipse at Tirunelveli (TNV), Braemore Hills (BMG) and Thiruvananthapuram (TVM)[a]

Meteorological Parameters and Stations	Morning Hours	Before Eclipse Period	During Eclipse Period	After Eclipse Period	Evening Period	Night
		Temperature (°C)				
TNV	24	27	24	30	27	23
BMG	25	28	25	25.5	28	23
TVM	25	31	27	31	32	22
		Wind direction				
TNV	N	N	NE	NE	NE	N
BMG	E	N	--	NE	ES	E
TVM	N	S	S	NW	NW	N
		Wind speed m/S				
TNV	3.	2	2	3	4	3
BMG	4	4	0	1	1	2
TVM	2	1	1	3	3	1
		Humidity (%)				
TNV	85	48	83	46	60	67
BMG	90	55	82	63	55	75
TVM	92	55	82	62	88	88

[a]TNV – Tirunelveli, BMG – Braemore Hills, TVM – Trivandrum.

terrain does not support vegetation. Corona current can thus be totally avoided. The seacoast (Gulf of Manner) is at a distance of 35 km. Because the nearest cities of Tirunelveli and Palayamkottai are 14 km away from the experiment site, anthropogenic pollution is very little. The experiment site is therefore suitable for atmospheric electric studies as reported by *Panneerselvam et al*. [2003] and *Anil Kumar et al*. [2009b].

[10] January is the coldest month in this region with an average temperature of 24°C; wind direction is northerly or northeasterly with less convective activity. During the eclipse period, the wind speed was less than 2 m/s, surface temperature varied from 23°C to 30°C, and relative humidity varied from 48% to 90%. There were four oktas of cloud, with slight fog coverage during the early morning hours. After 1030 IST (0500 UT) the sky became very clear until the late evening hours, and the prevailing wind was weak. The day was therefore considered as "fair-weather" for this study.

3. Experiments

[11] The measurements of the atmospheric electric parameters and meteorological parameters are described here. The electric current components include the conduction current, displacement current, Maxwell current, and convection current. The conduction current, which is mainly a direct current, constitutes the current due to the actual transport of electric charges under the influence of an electric potential. The displacement current is the fluctuating part of the current and it contains a spectra of frequencies; it does not involve any charge transport in the medium, but it exists on account of the time variation of the electric field in the medium. When the charge carriers are driven by air motion, the current is called the convection current. The convection current can occur in different directions and intensities depending on the space charge density, air movements, stability of the atmosphere, and gravity acting on charged particle suspensions. The sum of all these current components is described as the Maxwell current. The current components have been successfully measured in recent years to study atmospheric electrical parameters at the Tirunelveli site [e.g., *Panneerselvam et al*., 2003, 2007; *Anil Kumar et al*., 2009b].

[12] The ground-based sensors used for the current measurements include the Wilson's plate [*Israel*, 1973], horizontal long wire antenna [e.g., *Kasemir*, 1955; *Ruhnke*, 1969], and spherical shell in the form of two hollow hemispheres [*Burke and Few*, 1978]. In Wilson's plate setup, the current collector is in the form of a metal plate flush with the ground to avoid convection current, and is isolated by an insulator supported by Teflon rods; the values of the Relaxation Time constant time constant are sufficient enough to avoid the displacement current. As soon as the charged particles come in contact with the antennas, the electric field is indicated by the electrometers with OP-AMP, AD 549, which convert the current into voltage and are duly calibrated. The electrometer measures the current in the range of picoamperes with high feedback resistance. A buffer stage (LM308) is connected to the electrometer output. The output signals are filtered by a low-pass filter (3 dB) at the input of an analog-to-digital converter that is nearly 50 m away from the preamplifier. The filtered signal is fed to a high-resolution Windows-based data logging system. One minute averaging of the data is carried out during the analysis stage.

[13] The ground-based electric potential sensor includes a passive antenna [*Harrison*, 1997] at 1 m height. In addition, we used an electric field monitor (EFM-100) of around 30 km field of view. The instrument's details are available at info@boltek.com, which provides the important parameter of the height integrated electric field variation over the wide area on the eclipse path. All sensors were properly earthed and experiments were run without power interruption. The outputs from the sensors, after proper signal conditioning, were fed to a highly sensitive 8 channel windows based data logger based data logger. Details of the instruments were described by *Panneerselvam et al*. [2007] and *Anil Kumar et al*. [2009a].

[14] In addition, the automated weather instruments at Tirunelveli, and manual observations of wet and dry temperatures, visual scanning of cloud coverage, and visibility checking are used. The meteorological data of Thiruvananthapuram (8.29°N, 76.55°E, 01 m AMSL) and Braemore Hill (8.41°N, 76.59°E, 460 m AMSL) stations are also used.

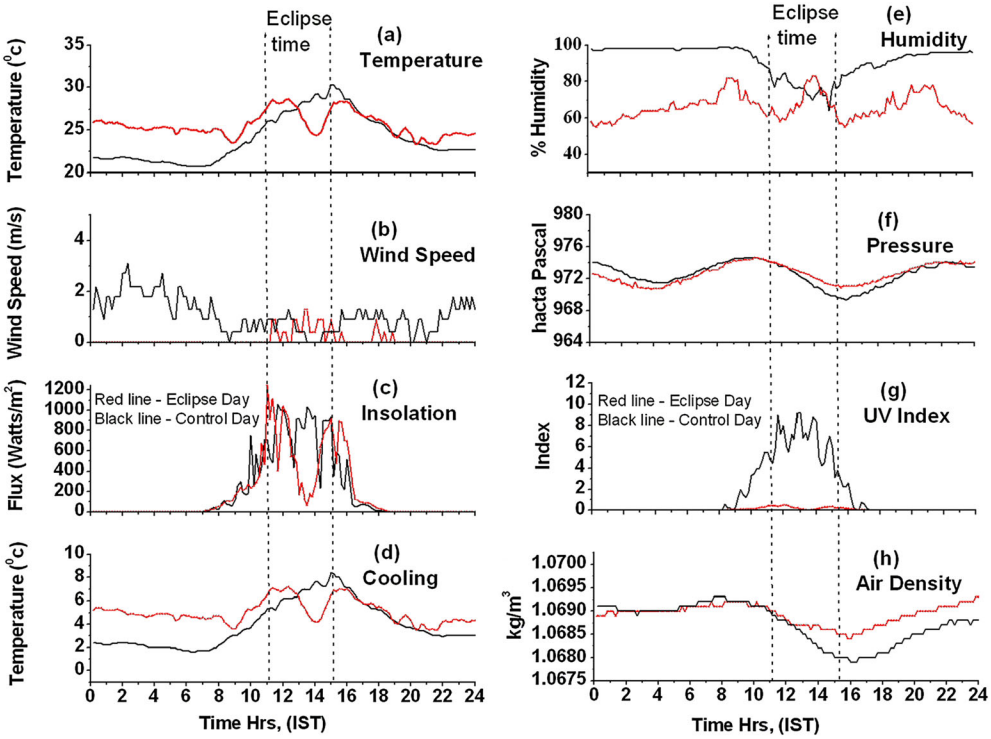

Figure 2. Red curves in the panels show the (a) surface temperature, (b) wind speed, (c) insolation, (d) rate of cooling, (e) humidity, (f) air pressure, (g) UV flux, and (h) air density measured on the solar eclipse day on 15 January 2010; vertical dotted lines show the eclipse window. Black curves show the corresponding parameters on control days.

[15] The data at Tirunelveli on the eclipse day are compared with the control data, which are the average data of five fair-weather days (1% standard deviation) in the same month (January 2010), section 4. Minute average data are used for the analysis. The manual meteorological observations from the three stations (Tirunelveli, Braemore Hills, and Thiruvananthapuram) during the eclipse are listed in Table 1. During the eclipse there was no rain, and visibility was good in all stations.

4. Results and Discussion

[16] The results are presented and discussed in this section. The variations of the meteorological parameters are presented in section 4.1. The meteorological fluctuations seem consistent with the variations of the atmospheric electric parameters described in section 4.2.

4.1. Micrometeorological Changes

[17] Figure 2 compares the variations of the meteorological parameters on the eclipse day (red curves) with those on control days (black curves). The eclipse window is shown by dotted lines. The manual meteorological observations at the three stations Tirunelveli (TNV), Braemore Hill (BMG), and Thiruvananthapuram (TVM) are listed in Table 1. As Figure 2 shows, the insolation (Figure 2c) decreased from about 1000 W/m^2 at the time of first contact to less than 100 W/m^2 at the peak of eclipse, a reduction of about 90%. The UV flux (Figure 2g), which has been low before the start of the eclipse for some reason, decreased to zero at the peak of the eclipse.

[18] Figure 2 also shows changes in all meteorological parameters. However, detectable changes started about an hour from the first contact (Figure 2), and peak changes also occurred about an hour after annularity. Except air density and air pressure, all other meteorological parameters recovered back to normal level soon after the end of the eclipse. As a consequence of the decrease in the short wave heating (insolation), the surface temperature decreases by up to 4°C (Figure 2a) and cooling increases by three units (Figure 2d). The level of humidity (Figure 2e) on control days is low during middaytime hours with a minimum at around 12:00–02:00 IST (black curve); however, on the eclipse day humidity as a whole (red curve) is low. Over the low level, as a consequence of the cooling, humidity rises by about 35%. The air density (Figure 2h) and air pressure (Figure 2f) on the eclipse day have been following those on control days until about an hour after the first contact. Afterward the density and pressure increase until the end of the eclipse; and while the pressure reduces to normal level by premidnight, density continues to remain high even after midnight. The wind speed (Figure 2b) has been nearly zero before the start of eclipse compared to a speed of up to 2 m/s on control days. However, during the eclipse the wind speed increases from zero to about 1 m/s. *Gray and Harrison* [2012] reported similar eclipse-induced wind changes during the eclipse of 11 August 1999. *Winkler et al*. [2001] reported transient turbulent mixing of the lower atmosphere during the same eclipse.

[19] Surface temperature is the most important indicator of thermodynamical processes in the atmosphere. The rapid decrease of air temperature (Figure 2) (rapid compared to

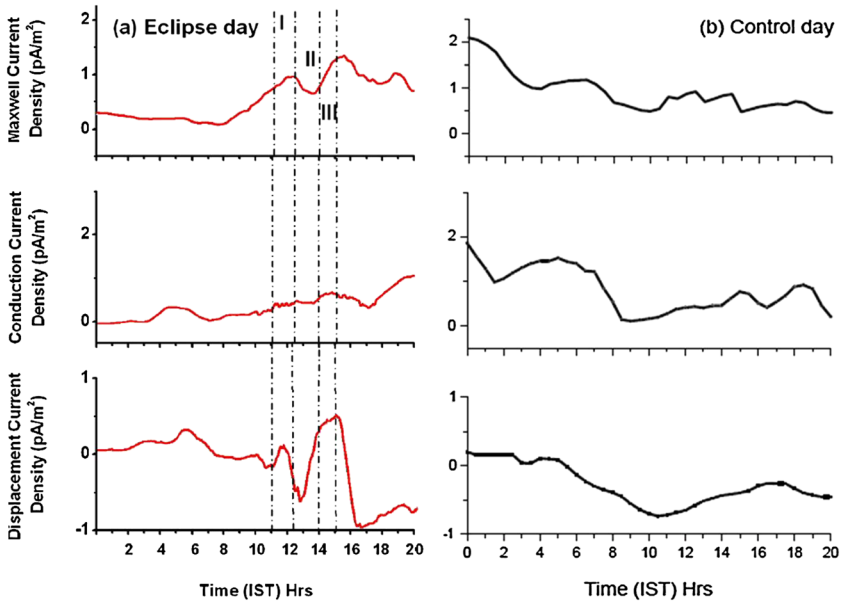

Figure 3. (a) Tracings of the original digital records of atmospheric currents during the solar eclipse on 15 January 2010; (top) Maxwell current (or total current), (middle) conduction current, and (bottom) displacement current. Stages I, II, and III illustrate the durations from first contact to annularity, second contact to third contact, and fourth contact to the end of the eclipse. At Tirunelveli eclipse started at 11:07:57 IST (05:37:57 UT), annularity was for about 8.5 min during 13:17:02–13:25:28 IST with maximum at 13:17:09 IST, and eclipse ended at 15:06:52 IST (09:36:52 UT); (b) similar to Figure 3a but for control or normal days.

nighttime cooling) causes the variations in humidity and air pressure that enable air parcels to move in advective and convective ways. Such air parcels with high/low free space charges can cause enhancement/reduction in the conductivity, and associated changes in electric potential, electric field, and electric current components as discussed in section 4.2.

4.2. Atmospheric Electric Parameters

[20] Figure 3 compares the variations of the different atmospheric current components measured at Tirunelveli on the eclipse day (left hand panels) with those on control days (right-hand panels). At Tirunelveli eclipse started at 11:07:57 IST (05:37:57 UT), annularity was for about 8.5 min during 13:17:02–13:25:28 IST with maximum at 13:17:09 IST, and eclipse ended at 15:06:52 IST (09:36:52 UT). The eclipse duration is classed as stage I (onset to start of annularity), stage II (duration of second and third contacts), and stage III duration from fourth contact to end of the eclipse; the stages are noted in Figure 3a. During the early morning hours on the eclipse day, fog prevailed until about 08:00 IST. Afterward the atmosphere became clear and total current gradually increased due to the increase in tropical convection.

[21] Comparing the eclipse and control data, the current components before the start of the eclipse differ significantly from those on control days, which may be part of the day-to-day variability of the currents. However, following the onset of the eclipse the currents start to fluctuate. The displacement current (Figure 3a, bottom panel) exhibits two large cyclic fluctuations within about 5 h from the start of the eclipse until about an hour after the end of the eclipse (sunset); and the period and amplitude of the fluctuations increase with the progress of the eclipse. The largest peak-to-peak amplitude is about 1 pA/m^2 with a peak negative current of about –0.5 pA/m^2 during stage II of the eclipse, and peak positive current of about 0.5 pA/m^2 by end of the eclipse (at around 15:06:52 IST). After the end of eclipse the current rapidly decreased and attained a phase change value of about –1 pA/m^2 in about an hour when the Sun set in the horizon, after which the current started a slow recovery.

[22] Similar fluctuations are also observed in Maxwell current, and to a lesser extent in conduction current (Figure 3a). The second cycle of fluctuation in the Maxwell current (top panel) that started at around the end of stage II seems to indicate that the surface air is uplifted through upward convection generated by solar heating after maximum eclipse. The convection current can occur in different directions and intensities; it also depends on the space charge density, air movements, stability of atmosphere, and gravity acting on charged particles' suspension. The fluctuations in the conduction current (middle panel) are weak; it may be because this current component generally depends on the global thunderstorm activity rather than on local generators.

[23] Figure 4 shows the electric conductivity (Figure 4a), electric potential (Figure 4b), and electric field (Figure 4c) variations on the eclipse day (red curves). The corresponding control-day data (black curve) are available only for the electric field. The eclipse window is shown by vertical arrows. As a result of the micrometeorological changes within the air (section 4.1), the small ions, which are more mobile than heavier ions, usually get attached to newly

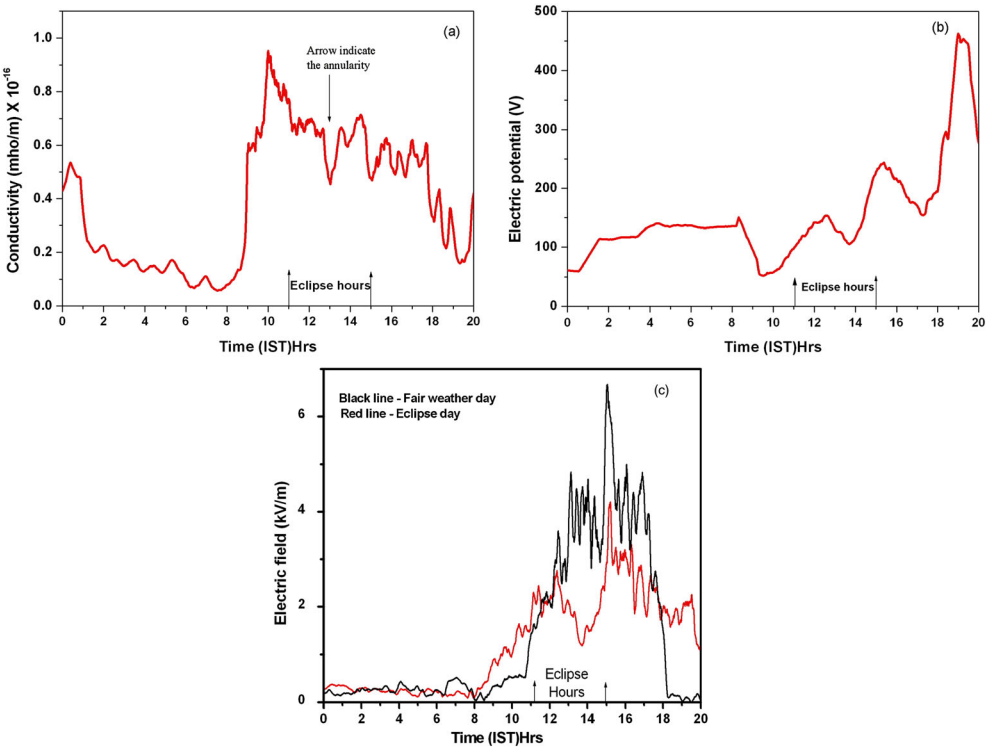

Figure 4. (a) Electric conductivity, (b) electric potential at 1 m height, (c) and ambient electric field measured on the solar eclipse day on 15 January 2012 (red curves); vertical arrows indicate eclipse window. The control days' data (black curve) are available only for electric potential (Figure 4c).

formed water droplets. This scavenging or coalescences process ends in free space charge reduction that can result in a large drop in the electric field centered at around the peak of the eclipse, and recovers toward normal level by the end of the eclipse. The measurements made by the atmospheric field monitor (EFM-100) seems to confirm the result (Figure 4c); compared to control-day data, the ambient electric field during the eclipse decreases by over 2.75 kV (over 65% decrease) in and around 30 km height integrated area. The process also seems to produce a small but sharp drop in the conductivity (Figure 4a) centered at the peak of the eclipse. However, the changes in the electric potential (Figure 4b), as recorded by the sensor at 1 m height, seems to be mixed with an unusual fluctuation that started before the eclipse and continues well after the eclipse; this resulted in three cyclic fluctuations, the strength of which continues to increase until sunset (Figure 4b).

[24] The data (Figure 4a) also seem to reveal the long-lasting paradox of conductivity enhancement during eclipse (the control-day data are not available). As shown by Figure 4a, the conductivity on the eclipse day undergoes the usual sharp increase in the morning at around 09:00 IST due to the increase in tropical convection. However, unlike on normal days, the conductivity undergoes a second increase just before the start of the eclipse, and high conductivity continues with fluctuations during the eclipse. The conductivity enhancement may be due to the eclipse induced upsurge of low winds and/or waves (cold front) that brings high density of free space charges embedded in air parcels. Such upsurge of wind speed just before an eclipse was reported [e.g., *Nymphas et al*., 2009].

[25] The eclipse induced variations of the electric parameters (Figures 3 and 4) are generally consistent with earlier studies, described in section 1. The enhancement of the currents that occurred soon after the peak of the eclipse (Figures 3a) may suggest that the total current begins to rise in accordance with local convection and enhanced circulation [e.g., *Anderson and Dolezalek*, 1972; *Szalowski*, 2002]. The build-up of the electric field after a large drop centered at the peak of the eclipse (Figure 4c) may also be caused by the posteclipse active convection due to the increased solar insolation enhancing the availability of free ions close to the ground; ions may also be released as drops get evaporated. The lunar orbital position may also reduce the intensity of galactic cosmic rays, which is a prime agent for ionization in the lower atmosphere except in the surface layer (or up to few tens of meters). This secondary reduction in the conductivity above the boundary layer may also be a factor for the fluctuations in total current and electric field.

[26] The cyclic fluctuations observed in the electric potential and currents extending well beyond the end of the eclipse (Figures 3 and 4) may also indicate the interactions of the eclipse-induced atmospheric changes and atmospheric electric properties. Eclipse-induced atmospheric waves were reported by several scientists. For example, *Farges et al*. [2003] detected the generation of gravity waves of 9–12 min period in atmospheric pressure. *Aplin and Harrison* [2003] observed 35 min period gravity waves in surface air pressure, which are interpreted as excited by the rapid cooling caused by the penumbra travelling at supersonic speed. A temperature decrease of up to 4°C within 2 h around midday (section 4.1) can affect the

stability of air and convective processes, which can provide favorable conditions for gravity wave generation.

5. Conclusions

[27] During the eclipse, significant decreases in Maxwell current and displacement current and electric field were observed. Our investigations support the view that, during the course of an eclipse, radiative cooling enables the formation and development of water droplets resulting in scavenging or coalescence of free ions/free space charges, which could cause the decreases in electric currents and fields; the reduction in galactic cosmic rays flux could also contribute to the decreases above the boundary layer. This scenario reverses after maximum obscuration and consequently the electric fields and currents return to normal levels. The observed UV flux reduction and micrometeorological changes such as in temperature, pressure, and density resulting in air mixing are associated with the eclipse. The observed conductivity enhancement is attributed to the variation in number-density of free ions or space charges in air parcel associated with the cold-front.

[28] **Acknowledgments.** This work was supported by the Department of Science and Technology (DST), Government of India.

References

Anderson, R. V. (1972), Atmospheric electricity, turbulence and pseudo-sunrise effect resulting from a solar eclipse, *J. Atmos. Terr. Phys.*, *34*, 567–572.

Anderson, R. V., and H. Dolezalek (1972), Atmospheric electrical measurements at Waldorf Maryland during the 7th March 1970 solar eclipse, *J. Atmos. Terr. Phys.*, *34*, 561–566.

Anil Kumar, C. P., R. Gopalsingh, C. Selvaraj, K. Jeeva, K. U. Nair, and S. Gurubaran (2009a), Atmospheric electric measurements at Dibrugargh during total solar Eclipse, *Scientific Report*, EGRL/IIG-SR-01/2009, 1-24.

Anil Kumar, C. P., C. Panneerselvam, K. U. Nair, K. Jeeva, C. Selvaraj, and S. Gurubaran (2009b), Measurement of Atmospheric Conduction Current Density from a tropical station using improvised Wilson's plate antenna, *Earth Planets Space*, *61*, 919–926.

Antonia, R. A., A. J. Chambers, D. Phorg-Anant, S. Rajagopalan, and K. R. Sreenivasan (1979), Response of atmospheric surface layer turbulence to a partial solar eclipse, *J. Geophys. Res.*, *84*, 1689–1692, doi:10.1029/JC084iC04pD1689.

Aplin, K. L., and R. G. Harrison (2003), Meteorological effects of the eclipse of 11 August 1999 in cloudy and clear conditions, *Proc. R. Soc. Lond. A*, *45*, 353–371.

Balan, N., B. V. Krishna Murthy, C. Raghava Reddy, P. B. Rao, and K. S. V. Subbarao (1982), Ionospheric disturbances during the total solar eclipse on 16 February 1980, *Proc. Ind. Nat. Sci. Acad.*, *48*, 43.

Burke, H. K., and A. A. Few (1978), Direct measurements of the atmospheric conduction current, *J. Geophys. Res.*, *83*, 3093–3098.

Chudzynski, S., et al. (2001), Observation of ozone concentration during the solar eclipse, *Atmos. Res.*, *57*(1), 43–47.

De, S. S., B. K. De, B. Bandyopadhyay, B. K. Sarkar, P. Suman, D. K. Haldar, S. Barui, D. Asim, P. Sam Sunder, and P. Nikhilesh (2010), The effects of solar eclipse of August 1, 2008 on Earth's atmospheric parameters, *Pre. Appli. Geophys.*, *167*, 1273–1279.

Deshpande, C. G., and A. K. Kamra (1992), Short time variations in atmospheric electrical parameters, *J. Atmos. Terr. Phys.*, *54*, 14213–1420.

Dhanokar, S., C. G. Deshpande, and A. K. Kamra (1989), Atmospheric electricity measurements at Pune during the solar eclipse of 18 Mach, 1988, *J. Atmos. Terr. Phys.*, *51*, 1031–1034.

Espenak, F., and J. Anderson (2010), Annular and total solar eclipses of 2010, NASA/TP-2008-21417.

Farges, T., A. Le Pichon, E. Blanc, S. Perez, and B. Al Coverro (2003), Response of the lower atmosphere and the ionosphere to eclipse of August, 1999, *J. Atmos. Sol. Terr. Phys.*, *65*, 717–726.

Gray, S. L., and R. G. Harrison (2012), Diagnosing eclipse–induced wind changes, *Proc. R. Soc. A: Math. Phys. Eng. Sci.*, *468*, 2143, 1839–1850, doi:10.1098/rspa.2012.2012.0007.

Harrison, R. G. (1997), An antenna electrometer system for atmospheric electric measurements, *Rev. Sci. Instrum.*, *68*(3), 1599–1603.

Israel, H. (1973), Atmospheric Electricity, Vol.II, Isr. Program for Sci. Transi., Jerusalem.

Jones, B. W. (1999), A search of atmospheric pressure waves from the total solar eclipse of 9 March 1997, *J. Atmos. Solar. Terr. Phys.*, *61*, 1017–1024.

Kamra, A. K. (1982), Fair weather space charge distribution in the lowest 2 m of the atmosphere, *J. Geophys. Res.*, *87*, 4257–4263, doi:10.1029/JC087iC06p04257.

Kamra, A. K., and N. C. Varshneya (1967), The effect of a solar eclipse on atmospheric potential gradient, *J. Atmos. Terr. Phys.*, *29*, 327–329.

Kamra, A. K., J. K. S. Teotia, and A. B. Sathe (1982), Measurements of electrical field and vertical distribution of space charge close to the ground during the solar eclipse of February 16, 1980, *J. Geophys. Res.*, *87*, 2057–2060, doi:10.1029/JC087iC03p02057.

Kasemir, H. W. (1955), Measurement of the air-earth current density, in Proc. Conf. Atmos. Electricity, Geophys. Res. Pap. 42, 91-95, Air Force Cambridge Res., Cent., Bedford.

Manohar, G. K., S. S. Kandalgaonkar, and M. K. Kulkarni (1995), Impact of a total solar eclipse on surface atmospheric electricity, *J. Geophys. Res.*, *100*, 20,805–20,814, doi:10.1029/95JD01295.

Nymphas, E. F., M. O. Adeniyi, M. A. Ayoola, and E. O. Oladiran (2009), Micrometeorological measurements in Nigeria during the total solar eclipse of 29 March, 2006, *J. Atmos. Sol. Terr. Phys.*, *71*, 1245–1253.

Panneerselvam, C., K. U. Nair, K. Jeeva, C. Selvaraj, S. Gurubaran, and R. Rajaram (2003), A comparative study of atmospheric Maxwell current and electric field from a low latitude station Tirunelveli, *Earth Planets Space*, *55*, 697–703.

Panneerselvam, C., C. Selvaraj, K. Jeeva, K. U. Nair, C. P. Anil Kumar and S. Gurubaran (2007), Diurnal variation of atmospheric Maxwell current over the low latitude continental station, Tirunelveli, *Earth Planets Space*, *59*(5), 429–435.

Radhakrishnan, E. P., N. Balan, A. A. Sridhar, and K. Usha Devi (1982), Effects of solar eclipse on shortwave transmissions, *Proc. Ind. Nat. Sci. Acad.*, *48*, 325.

Ruhnke, L. H. (1969), Area averaging of atmospheric electric currents, *J. Geomagn. Geoelectr.*, *21*, 453–462.

Saxena, D., and A. Kumar (2010), Measurements of atmospheric electric conductivities during the total solar eclipse of 22 July, 2009, *Ind. J. Phys.*, *84*(7), 783–788.

Szalowski, K. (2002), The effect of the solar eclipse on the air temperature near ground, *J. Atmos. Solar. Terr. Phys.*, *64*, 1589–1600.

Winkler, P., U. Kaminski, U. Kohler, J. Riedl, and H. Schroers (2001), Development of meteorological parameters and total ozone during the total solar eclipse of August 11, 1999, *Meterol. Z.*, *10*, 193–199.